X-RAY EMISSION FROM A LASER IRRADIATED TARGET IN THE PRESENCE OF HIGH ELECTRIC FIELD

S.G. DINEV, Ch.I. RADEV, K.V. STAMENOV and K.A. STANKOV
Department of Physics, Sofia University,
1126 Sofia, Bulgaria

Received 25 April 1979

The temporal characteristics of the X-ray emission from a laser irradiated Ai target in a 20 kV/cm electric field are measured with electronic detectors. Spatial and spectral distributions of the X-ray radiation are evaluated using a pinhole camera and filter technique.

1. Introduction

When an intense laser beam is focused on a solid target, an X-ray radiation from the laser plasma is emitted [1]. In order to obtain a high X-ray output high energy of the exciting pulse is needed – of order of joule or more for picosecond pulses [2–5] and tens of joules for nanosecond pulses [6–8]. Conversion efficiencies of 20–30% have been obtained using a laser system of 300 J in 1 ns [8]. An enhancement of the X-ray output of a laser irradiated target in a dc electric field was first reported by Farkas and Horvath [9]. In their recent experiment a strong increase in the X-ray emission has been recorded photographically when an Au target is inserted in a 20 kV/cm electric field.

In this paper we report the result of the detailed measurements of the X-ray pulses from a laser irradiated target influenced by a high dc electric field. Time characteristics of the X-ray emission were measured by means of electronic detectors and space distribution by a pinhole camera. The spectral content of the pulses was evaluated by filter technique.

The importance of this enhancement is obvious. The X-ray emission is an important tool for laser plasma parameter measurements. The spectral measurements give an information on the electronic structure of the highly ionized atoms [2,5,6]. Powerfull ultrashort pulses in the hard and soft X-ray region are now available only using high cost multistage laser systems with low repetition rate [8]. If such pulses are readily available with standard laboratory mode-locked lasers it will stimulate spectroscopic investigations in this region.

2. Experimental setu-up

The laser used in the measurements was a mode-locked Nd : glass laser L, fig. 1, with as main pulse parameters : pulse duration ~10 ps, number of pulses 20–25, interval between the pulses 10 ns. The fundamental radiation 1.06 μm was converted into its second harmonic in a KDP crystal in order to ensure optical isolation and higher efficiency in the multiphoton processes of laser beam interaction with the solid target. The green pulses of approximately 1 mJ energy of the individual pulse were focused by a 4.5 cm focal length lens O onto the surface of the target T. The glass lens is a window of the vacuum chamber and can be translated via micrometric screw and bellows. The target was a 5 mm thick aluminum plate with a purity better than 99% and a polished surface. The aluminum electrode E has a hole in the center to ensure a zero degree angle of incidence of the laser beam on the target. It is connected with the metal housing of the camera while the high voltage 0–60 kV from the power supply HVPS was applied through the

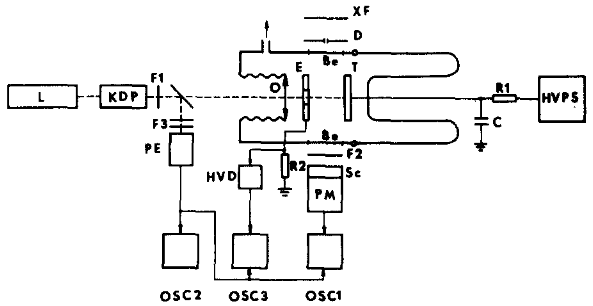

Fig. 1. Experimental set-up for measurement on X-ray emission parameters from an Al target in the presence of high electric field: L – mode-locked Nd : glass laser, KDP – crystal for second harmonic generation, O – focusing lens, T – target, E – electrode, Be – X-ray windows, D – pinhole, XF – X-ray photographic film, Sc – NE110 plastic scintillator, PM1 – FEU 36 photomultiplier, OSC1 – Tektronix 465 or 466 oscilloscope, PE – FEK 15 coaxial photoelement, OSC2 – C1-37 oscilloscope, HVD – high voltage divider, OSC3 – travelling wave oscilloscope, F1, F2 – optical glass and interference filters, F3 – X-ray filters, HVPS, high voltage power supply.

glass envelope to the target. The distance between the target T and electrode E is variable and was kept 15 mm during the experiment.

The resistance R1 = 1GΩ and capacitor C = 2.5 nF or 4.7 nF determined the peak current through the camera. The amplitude and the form of the current were measured on the 50 Ω load resistor R2 by a low inductance high voltage probe [10] with a risetime better than 0.1 ns and 1.5 GHz travelling wave oscilloscope I2-7.

The vacuum camera ‡ was evacuated to 10^{-6}–5×10^{-7} Torr. The X-ray radiation from the target was emitted through the 0.6 mm thick 15 mm in diameter Be windows, situated at 180°. The X-ray source was visualized by a ZOX-190T Chirana X-ray image intensifier (not shown on the figure). The space distribution of the emitting source was measured by a pinhole camera made by 0.5 mm in diameter hole in a 2 mm Pb plate D and an X-ray film XF. Time characteristic data were measured with NS 110 plastic scintillator Sc with 10 mm thickness, FEU-36 photomultiplier PM1 and Tektronix 465 or Tektronix 466 oscilloscope OSC1. The scintillator–photomultiplier system was protected from light by a 0.6 mm Be foil. Laser beam fluctuations at the entrance window were monitored by a FEK-15 coaxial photoelement PE and storage oscilloscope OSC2. The FEK-15 (0.3 ns rise time) signal was also used for triggering the OSC1 and OSC2 oscilloscope.

‡ Modified BSV-2 crystallographic X-ray tube.

3. Space distribution measurements

First, the optimum focusing position of the lens O was determined monitoring the X-ray flux.

With a negative polarity of the high voltage on the target a large diffuse spot was seen on the ZOX-190T screen and on the photographic plate, originating from the target surface. In this case the camera acts as a fast X-ray tube with initial electrons from the laser plasma.

Next, a positive voltage was applied to the target. We have concentrated on this polarity and it will be kept in all measurements to be described. When a 0.5 mm diaphragm was inserted in front of the X-ray image intensifier, an elliptical spot could be seen. In order to determine the position and the form of the emitting source several pinholes were tried ranging in diameter from 0.05 mm to 0.5 mm. A run of 150 shots at 25 kV and 0.5 mm pinhole were needed to get the proper photographic exposure. On the photographic plate besides the diffuse elliptical spot emitted from the target surface a small concentrated spot was superimposed in the center in agreement with [9]. Series of photographs were made when besides the 0.5 mm pinhole an additional 3 mm diameter hole was made. In this way the sharp edge of the shadow showed the exact position of the target plane. Following [11] with a pinhole diameter a = 0.5 mm, object distance u = 30 mm, image distance v = 43 mm, we obtained from the microdensitograms of the pinhole camera pictures a point-like source less than 1 mm in diameter (limited by the resolution of the pinhole camera) within 1 mm from the target surface. Evidently the origin of the emission is in the laser plasma. The form of the spot can be seen on fig. 2, where an equidensitogram of the X-ray source is shown. From the equidensitogram on fig. 2 a typical asymmetry in the Y axis, the direction of the laser beam, is seen. The steeper slope on the target side can be explained by the gradient in the expanding plasma, formed in the strong electric field. The asymmetry in the X-axis is not typical for all pinhole camera pictures and is probably due to an

Fig. 2. Equidensitogram of the X-ray point-like source.

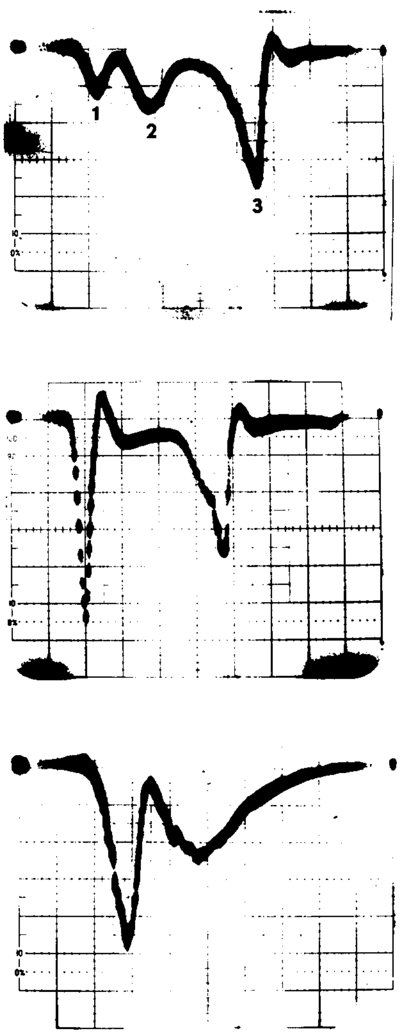

Fig. 3. Oscillogram of the X-ray pulses, a) R1 = 0, C ≠ 0, first, second and third pulses presented, b) R1 = 0, C ≠ 0, first and third pulses, c) R1 = 1 GΩ, C = 0, first and second pulses. Horizontal scale 100 ns/div, vertical scale 0.2 V/div.

asymmetry in the focusing geometry and in the laser drilled pinhole.

4. Time resolved measurements

The temporal response of the scintillator, photomultiplier, and the oscilloscope are comparable and are of the order of several nanoseconds. When exposed to the laser pulses the photomultiplier displayed a clear pulse train with ~100% modulation. The measured FWHM of a single electron pulse, obtained with ^{57}Co γ-source, is 10 ns.

A typical form of the X-ray pulses on the Tektronix 466 storage screen is shown on fig. 3. As seen from fig. 3a, made at R1 = 0, three pulses called 1, 2 and 3 within 1 μs are presented. The delay time position of the first pulse 1 with a mean duration of 40 ns is very stable and its maximum coincides with the maximum of the laser pulse train. The amplitude of the second

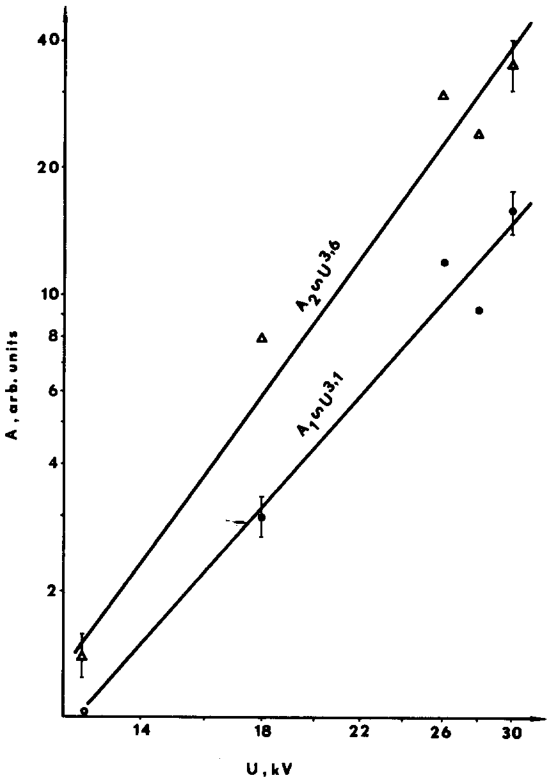

Fig. 4. Amplitude versus voltage dependence of the X-ray pulses at R1 = 0, ○ first pulse, △ second pulse.

Table 1
Delay time dependence of the second pulse $\tau_2 \sim U^{a_2}$ and the third pulse $\tau_3 \sim U^{a_3}$ on the applied voltage U for different values of C.

C nF	0	1.5	4.8
a_2	−0.48	−1.77	−3.65
a_3	–	−1.37	−1.92

pulse depends on the amplitude of the first one and in the case of high enough amplitude of the latter it almost disappears, fig. 3b. The third pulse is presented only at R1 = 0, fig. 3a, b, c. The amplitude of the pulses depends in different way on the magnitude of the applied positive voltage on the target, fig. 4. Within the experimental error the powers in the dependence $A \sim U$ do not depend on the peak current (increasing the value of the capacitor C).

The position of the second and the third pulses in reference to the first one also depends on the magnitude of the applied voltage, table 1. However, as seen from the table, this dependence is going steeper with the increase of the peak current.

5. Spectral evaluation

A two millimeter Pb plate completely stops the image on the ZOX-190T screen and all three pulses on the scope. Filter foils of different materials – Al, V, Mn, Ni, and Zr with K-absorption edges ranging from 8.33 Å to 0.69 Å caused a little change in the image visibility on the X-ray image intensifier, showing the presence of hard components with energy ⩾20 keV. The absorption of the three pulses by the filters is different. The relative absorption, say in V filter with a K-edge 2.26 Å, is 2.4 for the first pulse, 1.2 for the second, and 1 for the third one.

A rough estimate from the collected filter data shows that the first pulse has mostly soft components of the order of 15 keV. Softer components could not be recorded due to the thick Be windows.

6. Form of the current pulses

The form of the current on the 50 Ω load resistor R2 was measured with an overall time resolution better than 1 ns. A train of high-voltage nanosecond pulses with a repetition rate coinciding with the laser pulse train was followed by a long pulse several tens of nanoseconds in durations, in agreement with [9]. The amplitude of both short and long pulses was several kilovolts.

7. Discussion

When picosecond laser pulses with an intensity of $\sim 5 \times 10^{12}$ W/cm^2 were focused onto a solid Al target in an electric field ~20 kV/cm, an increase of several orders of magnitude in the X-ray emission was recorded.

Keeping in mind the main characteristics of the three pulses, the following mechanisms in our view can take place:

1) The first pulse, which coincides with the laser pulse train and is accompanied by short current pulses of high amplitude can be cause by recombination, bremsstrahlung and line radiation from the highly ionized laser plasma. The strong enhancement caused by the electric field is probably due to the higher ionization cross-section [12,13], which at 20 kV/cm may be orders of magnitude increased. Thus the absorption and hence the plasma temperature is enhanced. An experiment is now under way to record the spectrum of the radiation.

2) The second pulses is delayed according to the law $\tau_3 \sim U^{-0.48}$ (table 1) when an electric field is applied without discharge of a capacitor. Within the experimental error it is in a good agreement with the prediction for an X-ray pulse following the ionic bombardment of the electrode E and consequent emission of electrons, accelerated toward target T [1]. The enhanced dependence on the magnitude of the applied voltage when the low inductance capacitor is increased is difficult to explain.

3) The third pulse has high energetic components and evidently is presented only when a capacitor is discharged in vacuum.

More experimental data is needed to clear out all mechanisms for the enhanced X-ray production.

Acknowledgements

The authors are greatly indebted to Prof. F. Bunkin for helpful discussions and interest to the work. Thanks are also due to Dr. S. Vladimirov for the excellent equidensitograms, K. Burin and E. Vapirev for the help in the experiment.

References

[1] J.F. Ready, Effects of high power laser radiation (Academic Press, New York – London, 1971).
[2] M.A. Khan, D. Jacoby and G.J. Pert, Optics Comm. 20 (1977) 89.
[3] M.H. Tuillier and B. Lacour, J. Phys. B: Atom. Molec. Phys. 10 (1977) 1407.
[4] B. Luther-Davis, Optics Comm. 23 (1977) 98.
[5] E.V. Aglitsky, A.N. Zherikhin, P.G. Kriukov and S.V. Chekalin, Optics Comm. 20 (1977) 86.
[6] V.A. Bojko, S.A. Picus, I.U. Safronova and A.J. Faenov, Kvantovaya electronika 4 (1977) 600.
[7] J.C. Couturand, Optics Comm. 22 (1977) 71.
[8] P.J. Mallozzi, H.M. Epstein, R.G. Jung, D.C. Applebaum, B.P. Fairand and W.J. Callagher, X-ray emission from laser generated plasmas, in: Fundamental and applied laser physics, Proc. of the Esfahan Symposium, 1971 (John Wiley and Sons) p. 165.
[9] Gy. Farkas and Z.Gy. Horvath, Optics Comm. 21 (1977) 408.
[10] C.E. Violet, Instrumentation for X-ray diagnostics of plasma, in: Advances in X-ray analysis, vol. 18, eds. W.L. Pickles, C.S. Barrett, J.B. Newkirk and C.O. Ruud (Plenum Press, New York) p. 26.
[11] V.S. Letokhov, V.I. Mishin and A.A. Puretzky, Progress in Quantum Electronics 5 (1977) part 3, 139.
[12] R.V. Ambartzumian, G.I. Bekov, V.S. Letokhov and V.I. Mishin, Pisma Zh. Exp. i Teor. Fiz. 21 (1975) 595.